Preliminary Study of Cooling Performance on Metal Containment Vessel design with Thermal Radiation Shielding for Application of Small Modular Reactor Development

Geunyoung Byeon [a], Namgook Kim[a], Beomjin Jung [a], Geon Hyeong Lee [a], Sung Joong Kim [a,b*]
[a]*Department of Nuclear Engineering Hanyang Univ., 222, Wangsimni-ro, Seongdong-gu Seoul, Korea*
[b]*Institute of Nano Science and Technology, Hanyang Univ., 222 Wangsimni-ro, Seongdong-gu, Seoul, Korea*
[*]*Corresponding author: sungjkim@hanyang.ac.kr*

Keywords: Heat Transfer, Heat loss, Metal Containment Vessel (MCV), Small Modular Reactor (SMR)

1. Introduction

Small modular reactors (SMR) have gained prominence on the global stage owing to its enhanced safety features, compact and simple design, and the potential to cater to diverse industrial applications beyond electricity generation [1-2]. SMRs under global development exhibit innovative designs such as integrated nuclear steam supply system (NSSS). Among them, the noteworthy structure of the SMR includes a metal containment vessel (MCV) structure. The MCV surrounding a reactor pressure vessel (RPV) could withstand a higher design pressure than concrete containment. Moreover, it could prevent over-pressurization by either flooding the outside of the metal containment with water or installing a separate heat exchanger [3].

The gap located between the RPV and the MCV could also play a significant role by acting as an extra barrier reducing heat loss to exterior of the RPV. The effectiveness of heat loss reduction can differ based on the condition of the gas filled within the gap. Among the various filling conditions in the gap, vacuum condition in the gap may be considered best due to a minimized convective heat transfer during normal operation and an enhanced condensation performance based on the lower concentration of a non-condensable gases during transient state [4]. Nonetheless, our previous computational fluid dynamics (CFD) investigations have revealed that the most dominant heat transfer mechanism is not a conductive and convective heat transfer but a radiative heat transfer [5]. From this perspective, despite the advantageous characteristics of the vacuum filling, the installation of shielding within the gap appears to be worth considering regarding the reduction of heat loss during steady-state conditions.

However, the radiation shielding intended to contribute to the reduction of the heat loss has the potential to degrade a steam condensation performance, which is a major factor during reactor transient condition, by acting as a kind of the flow barrier. Moreover, the shielding could limit the behavior of steam that contacts the MCV, which acts as a heat sink, potentially compromising cooling efficiency. Therefore, it becomes necessary to evaluate the cooling performance with installing shielding under transient conditions.

In terms of this, the aim of this study, the cooling performance within the MCV was assessed based on the presence or absence of shielding. Furthermore, in cases where shielding was present, the effect of shielding diameter and roughness was investigated.

2. Heat Loss Experiment at Transient State with Thermal Radiation Shielding

2.1 Experimental Apparatus

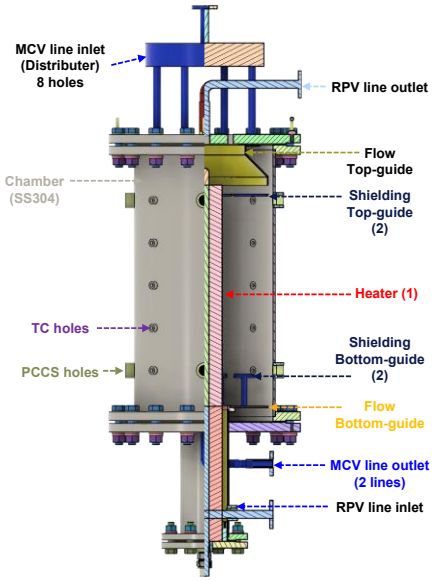

Fig. 1. Cross-section of a conjugate heat transfer experimental apparatus.

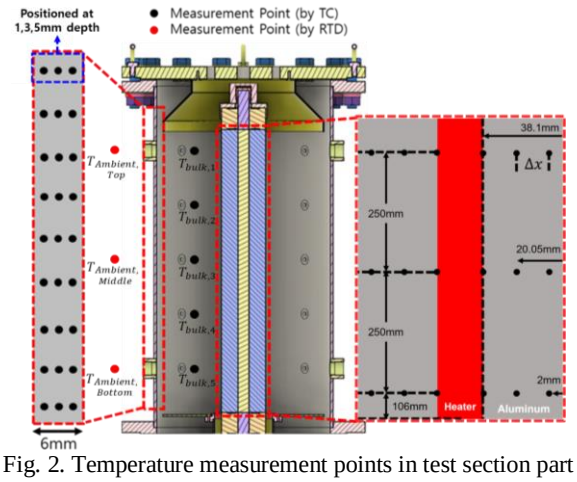

Fig. 2. Temperature measurement points in test section part

Figure 1 illustrates the experimental setup designed for conjugate heat transfer, which simulates the MCV. This arrangement assesses the total heat losses attributed to various heat transfer mechanisms in both reactor steady states and transient conditions involving condensation heat transfer within the MCV.

At the core of the chamber, there is a heater (0.0254m diameter, 0.85m length), encircled by an aluminum conductor (0.1016m outer diameter) to replicate the RPV heat emission. The experimental chamber section measures 0.406m in outer diameter and 0.815m in height. The choice of the outer diameter corresponds to a crucial factor in radiative heat transfer experiments, known as the view factor (F=0.273), which harmonizes with the geometries of the pressurizer and containment vessel being developed by KOREA HYDRO & NUCLEAR POWER i-SMR design. The lower chamber section incorporates guide structures for thermal radiation shielding, accommodating shielding diameters of 0.2m, 0.3m, and 0.4m.

Pressure transmitters at the top of the chamber measure its pressure. The heater, as shown in Figure 2, is equipped with three K-type thermocouples (TC) at different heights and depths. Additionally, as depicted in Figure 2, five TCs are positioned at varying heights to measure the Bulk Temperature at the midpoint of the chamber's inner diameter. Inside the MCV, thermocouples are distributed by height and depth, while three RTDs measure the ambient temperature outside the MCV.

2.2 Test Matrix

In this experiment, the cooling performance of the steam discharged from the automatic depressurization valve (ADV) to the MCV was evaluated by assuming a scenario in which the ADV became stuck open after normal operation.

To establish the initial condition of the steam ejection, preliminary MELCOR analysis was conducted, which considered the changes over time in water level and the mass discharge of water/steam from the ADV in actual scale scenarios of the 540 MW_{th} reactor [6]. However, it should be noted that the used MELCOR input assumed air as the internal filling material within the MCV. Therefore, for this vacuum-based experiment, the total quantity of the ejected steam was determined by using the steam mole fraction from MELCOR results (eq. (1) and (2)).

$$W_{air} = \frac{P_{air}M_{air}}{P_{air}M_{air} + P_{steam}M_{steam}} \quad (1)$$

$$X_{steam} = \frac{W_{steam}/M_{steam}}{W_{steam}/M_{steam} + W_{air}/M_{air}} \quad (2)$$

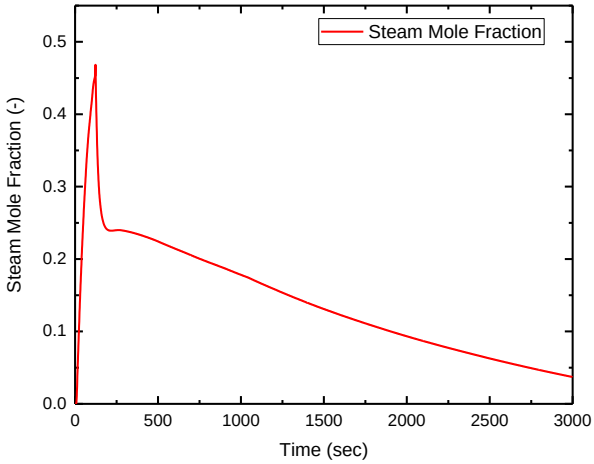

Fig. 3. Mole fraction variation within MCV over time. (MELCOR result)

The maximum steam mole fraction within the MCV was determined to be approximately 0.47, as shown in Figure 3. From the resultant steam mole fraction and the scaling law, the steam of 0.32 kg was injected during the experiment.

For the heater temperature, it was set to 320°C, which was determined based on previous CFD research [5] as the temperature of the pressurizer section. The ambient temperature was set to room temperature (~18°C). The pressure was set to 0.07 bar, which is the nominal operating pressure of the containment in the NuScale SMR with a vacuum gap condition [9].

The material utilized for the shielding in this experiment is SUS304, with a thickness of 0.3mm. In radiative heat transfer, previous research has indicated that, when temperature and emissivity remain constant, the most influential factor is the view factor, which is mainly affected by the gap distance [7]. Additionally, studies have highlighted that even specimens made of the same material can exhibit varying emissivity due to differences in surface roughness [8]. In this regard, this study adopted the shielding diameter and the surface roughness as manipulated variables of the manipulated variables of the experiment.

The test matrix of this study applying the above variables is shown in Table I below.

Table I: Test Matrix

Heater Temperature	320 °C
Ambient Temperature	18 °C
Injected Steam Mass	~ 0.32 kg
Injected Steam Temperature	~ 145 °C
Initial Pressure	0.07 bar
Shielding Condition	Case I (w/o Shielding)
	Case II (D200, G2400)
	Case III (D400, G2400)
	Case IV (D400, G40)

3. Results and Discussion

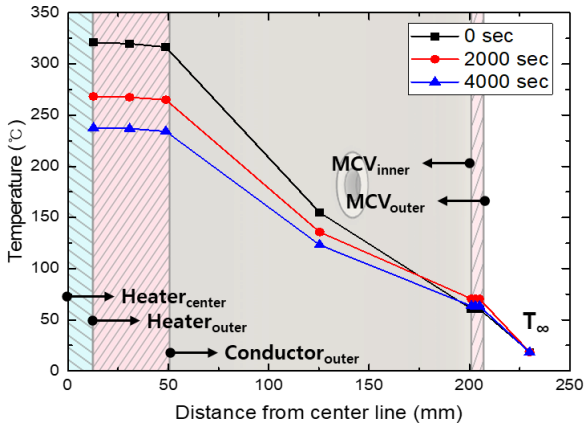

Fig. 4. Temperature distribution in Case I in the upper region

The temperature distribution measured in Case I (w/o shielding) at different time points of 0, 2000, and 4000 sec after steam injection is shown in Figure 4. As time elapses, it becomes evident that both heater and bulk temperatures decrease. However, the MCV temperature experiences an initial rise due to steam-induced heating, followed by a cooling trend as time progresses, resulting in a decrease in temperature.

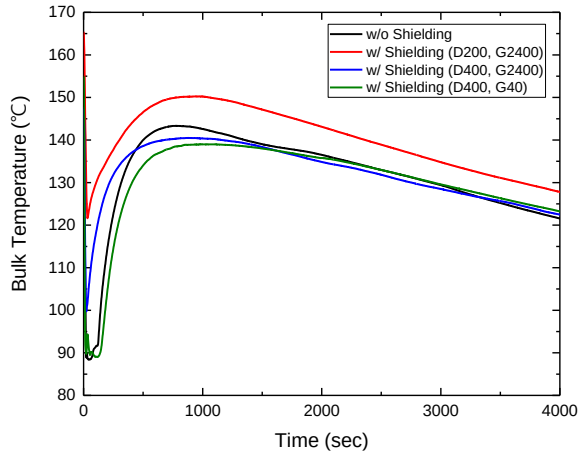

Fig. 5. Bulk temperature in upper region.

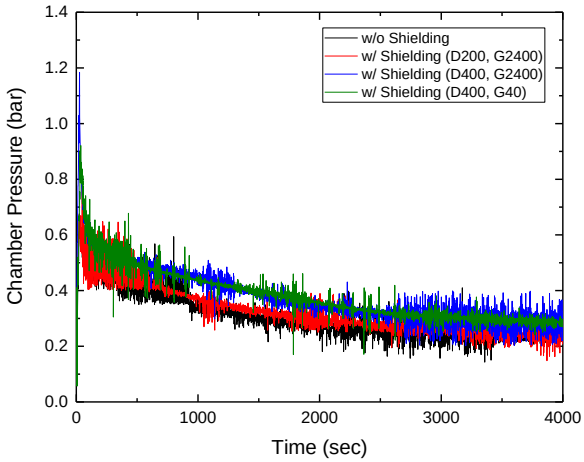

Fig. 6. Pressure in chamber.

Figure 5 and Figure 6 illustrate the bulk temperature and the pressure in the upper region of the chamber, respectively. In Figure 5, there is a sharp temperature decrease as steam is injected. This phenomenon can be attributed to the adiabatic expansion of the chamber, where the volume of the chamber rapidly increases compared to the volume of the steam generation line. As a result of this expansion, the temperature could drop. In Figure 6, the pressure graph shows that the pressures are initially the same during the steam injection. However, it can be observed that the rate of pressure decrease varies for each case.

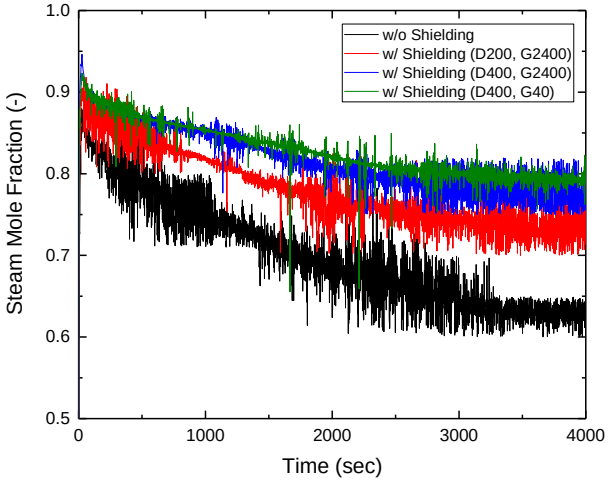

Fig. 7. Calculated steam mole fraction

In order to evaluate the cooling performance of each test cases, the steam mole fraction is calculated from the closed-chamber pressure and the bulk temperature according to eq. (2) as shown in Figure 7. The resultant steam mole fraction shows the continuous decrease during the measured experimental time, which means that there is a continuous phase change from the steam to the condensed water.

From the perspective of shielding presence, it can be observed that Case I (w/o shielding) exhibit consistently lower steam mole fractions throughout all time steps when compared to other cases with shielding. This indicates that condensation of steam within the chamber is more effective in cases with shielding, implying superior cooling performance due to enhanced condensation.

Specifically, regarding the shielding diameter, a comparison between Case II (D200, G2400) and Case III (D400, G2400) reveals that the steam mole fraction in Case II, with a smaller shielding diameter, is consistently lower than in Case III throughout all time steps. This suggests that the shielding hampers the reach of steam to the MCV surface, which acts as a heat sink, leading to reduced condensation heat transfer within the chamber. Therefore, it can be concluded that a smaller shielding diameter near the MCV leads to compromised cooling performance.

When considering the aspect of shielding roughness, a comparison between Case III (D400, G2400) and Case IV (D400, G40) demonstrates minimal differences throughout the entire time. This implies that there is little variation in cooling performance between these cases.

Ultimately, the installation of shielding allows for the discernment that the most dominant influence on cooling performance lies in the shielding geometry.

4. Conclusion

In this study, a preliminary experiment was executed to assess the cooling performance, incorporating variables such as the presence of radiation shielding, shielding diameter, and shielding surface roughness. The experimental setup, emulating the MCV, provided valuable insights into heat loss mechanisms across both steady-state and transient conditions, emphasizing condensation heat transfer. Evaluating steam cooling performance through an ADV stuck-open scenario post-normal operation, we discovered that the absence of shielding (Case I and Case II) resulted in superior cooling performance, evidenced by changes in the steam mole fraction calculated from the measured pressure and bulk temperature. The interference caused by shielding, with varying diameters and roughness, effectively impeded heat removal from the MCV wall, thus hindering steam heat transfer. Crucially, our findings underscore that, in terms of cooling performance, the primary influencer is the geometry of the shielding itself. In conclusion, this study offers crucial insights for optimizing the cooling performance of SMRs under transient conditions, with a focus on the pivotal role played by shielding geometry.

5. Acknowledgement

This study was sponsored by the Korea Hydro & Nuclear Power Co.’s affiliated Central Research Institute (KHNP-CRI).

REFERENCES

[1]. M.D. Carelli et al., "Economic features of integral, modular, small-to-medium size reactors," Progress in Nuclear Energy, 52 (4), pp. 403-414 (2010).
[2]. D.T. Ingresoll et al., "NuScale small modular reactor for Co-generation of electricty and water," Desalination, 340, pp. 84-93 (2014).
[3]. H. Subki, “ADVANCES IN SMALL MODULAR REACTOR TECHNOLOGY DEVELOPMENTS”, 11, IAEA, Vienna, and Austria (2022).
[4]. Reyes Jr, José N. "NuScale plant safety in response to extreme events." Nuclear Technology 178.2 (2012): 153-163.
[5]. G. H. Lee et al., “CFD Evaluation of Radiative and Natural Convective Conjugate Heat Transfer in the Gap Space between Small Modular Reactor Vessel and Metal Containment during Normal Operation”, Transactions of the Korean Nuclear Society Autumn meeting, pp.1 – 5 (2022)
[6]. C. H. Song et al., “MELCOR Analysis of Core Coolability by Flooding Safety System Applicable for i-SMR”, Transactions of the Korean Nuclear Society Spring meeting, pp.1-5 (2023)
[7]. Barforoush, Mohammad Sadegh Motaghedi, and Seyfolah Saedodin. "Heat transfer reduction between two finite concentric cylinders using radiation shields; Experimental and numerical studies." International Communications in Heat and Mass Transfer 65 (2015): 94-102.
[8]. Jo, HangJin, et al. "Spectral emissivity of oxidized and roughened metal surfaces." International Journal of Heat and Mass Transfer 115 (2017): 1065-1071.
[9]. NuScale Power, L. L. C. "Status Report–NuScale SMR." (2020).